Progress In Electromagnetics Research Letters, Vol. 29, 185–199, 2012

DESIGN AND DEVELOPMENT OF CORNER TRUNCATED *U* AND INVERTED U-SLOT MULTIBAND TUNABLE RECTANGULAR MICROSTRIP ANTENNA

N. Kulkarni*, S. N. Mulgi, and S. K. Satnoor

Department of PG Studies and Research in Applied Electronics, Gulbarga University, Gulbarga-585106, Karnataka, India

Abstract—This paper presents the design and development of corner truncated rectangular microstrip antenna comprising *U* and inverted U-slot for multiband tunable operation, wide impedance bandwidth, and high gain. By incorporating *U* and inverted U-slots of optimum geometry on the radiating patch the proposed antenna operates between 3 to 12 GHz at different frequency bands and giving a peak gain of 1.73 dB without changing the nature of broadside radiation characteristics, compared to conventional rectangular microstrip antenna. The experimental and simulated results are in good agreement with each other. Design concepts of the antenna are given. The experimental results are presented and discussed. The proposed antennas may find applications in WiMax, HIPERLAN/2, and radar communication systems.

1. INTRODUCTION

Microstrip antennas (MSAs) have become widespread because of their attractive features such as planar, light weight, low profile, easy fabrication, compatibility with microwave, and millimeter-wave integrated circuits, low production cost [1] etc. Modern communication systems, such as WiMax, HIPERLAN/2 and radar communication [2, 3], often require antennas possessing two or more discrete frequency bands with considerable impedance bandwidth and adequate gain, which can avoid the use of multiple antennas. Hence it has become interesting area for the microstrip antenna designer to meet these requirements. The techniques available in the literature to improve the impedance bandwidth are the use of materials with

Received 28 November 2011, Accepted 9 January 2012, Scheduled 8 February 2012
* Corresponding author: Nagraj Kulkarni (nag_kulb@rediffmail.com).

low dielectric constants, thicker substrates, use of impedance matching networks, multi resonators, multi layer structures and utilizing the air gap between the layers, meandered ground plane, slot loading, stacked shorted patch, feed modification [4–14], etc. Also, the methods proposed in the literature to enhance the gain of microstrip antennas use parasitic patch, array antenna [15, 16], etc. These methods are effective at the cost of increased size of the antenna. The demand of multiband antennas is fulfilled by cutting slots of different geometries, such as bow-tie, rectangular, square ring, annular ring, on the radiating patch [17–20]. But a single antenna having wide impedance bandwidth and better gain with tunable multibands property is found to be rare in the literature.

2. DESIGNING

The proposed antennas are designed and developed using low cost glass epoxy substrate material of thickness $h = 1.66$ mm and dielectric constant $\varepsilon_r = 4.2$. The artwork of proposed antennas is sketched using computer software Auto CAD to achieve better accuracy. Photolithography process is used to fabricate the antennas. The bottom surface of the substrate consists of a tight ground plane copper shielding.

Figure 1 shows the top view geometry of conventional rectangular microstrip antenna (CRMSA). This antenna is designed for the

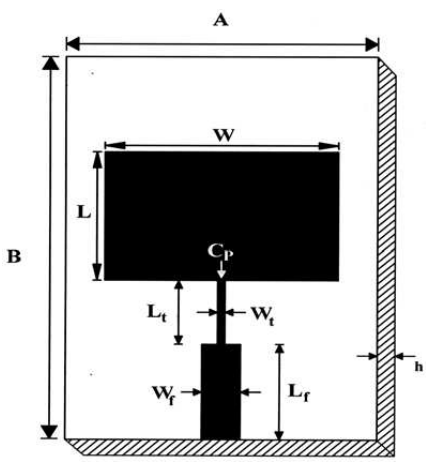

Figure 1. Top view geometry of CRMSA.

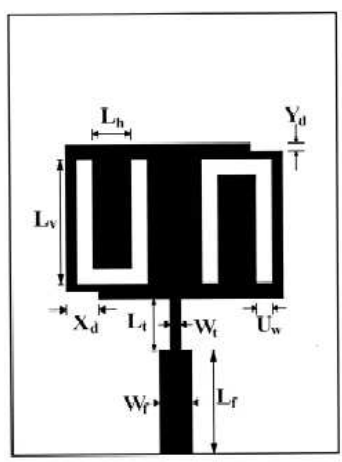

Figure 2. Top view geometry of CTUAIURMSA.

resonant frequency of 3.5 GHz using the equations available in the literature for the design of rectangular microstrip antenna on the substrate area $A \times B$ [21]. CRMSA consists of a radiating patch of length L and width W. The radiating patch is excited through a microstripline of length L_f and width W_f. A 50 Ω semi miniature-A (SMA) connector is used at the tip of the microstripline to feed the microwave power. A quarter wave transformer of length L_t and width W_t is incorporated to match the impedances between C_P and microstripline feed.

Figure 2 shows the top view geometry of corner truncated U and inverted U slot rectangular microstrip antenna (CTUAIURMSA) which is constructed from CRMSA. Two opposite corners along the width of CRMSA are truncated as X_d and Y_d. The novel U and inverted U slots are place symmetrically on either side from the center of the rectangular radiating patch. The dimension of U and inverted U slots are kept equal. L_h and L_v are the lengths of horizontal and vertical arms of U and inverted U slots, respectively. The dimensions L_h and L_v are taken in terms of λ_0, where λ_0 is a free space wave length in cm corresponding to the designed frequency of 3.5 GHz. U_w is the width of horizontal and vertical arms of U and inverted U slots. The U

Table 1. Design parameters of CRMSA and CTUAIURMSA (in cm).

$L = 2.04$	$W = 2.66$
$L_f = 2.18$	$W_f = 0.32$
$L_t = 1.09$	$W_t = 0.06$
$X_d = 0.8$	$L_h = \lambda_0/85$
$Y_d = 0.2$	$L_v = \lambda_0/42$
	$A = 5$
	$B = 8$

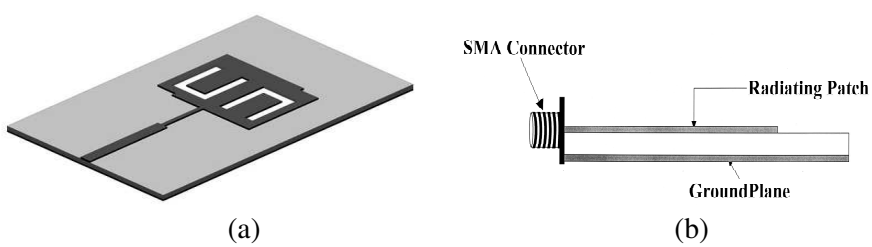

Figure 3. 3D view and side view of CTUAIURMSA. (a) 3D view of CTUAIURMSA. (b) Side view of CTUAIURMSA.

and inverted U slots are placed at a distance of 0.25 cm and 0.305 cm from non-radiating (L) and radiating (W) edges of the rectangular patch respectively. The various dimensions of the proposed antennas are listed as in Table 1. Figures 3(a) and (b) show the 3D view and side view of CTUAIURMSA respectively.

3. EXPERIMENTAL RESULTS

The Rohde and Schwarz, German make ZVK model 1127.8651 Vector Network Analyzer is used to measure the experimental return loss of CRMSA and CTUAIURMSA. The simulation of the CRMSA and CTUAIURMSA is carried out using Ansoft High frequency structure simulator (HFSS) software.

Figure 4 shows the variation of return loss versus frequency of CRMSA. From this figure it is seen that the CRMSA resonates at 3.39 GHz of frequency which is close to the designed frequency of 3.5 GHz. The experimental impedance bandwidth over return loss less than -10 dB is calculated using the formula,

$$\text{Impedance bandwidth}\,(\%) = \frac{f_2 - f_1}{f_c} \times 100 \tag{1}$$

where f_2 and f_1 are the upper and lower cut off frequencies of the resonating band when its return loss reaches -10 dB, and f_c is a centre

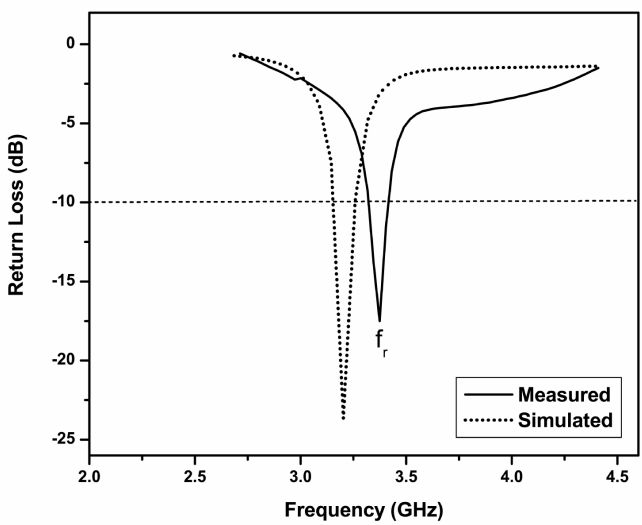

Figure 4. Variation of return loss versus frequency of CRMSA.

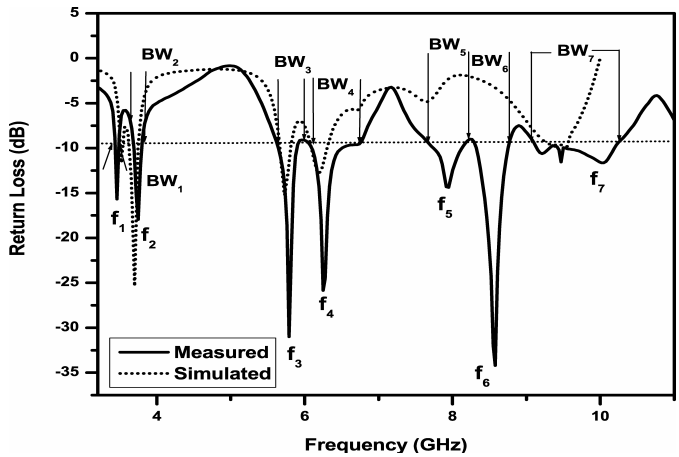

Figure 5. Variation of return loss versus frequency of CTUAIURMSA when $U_w = 0.2\,\text{cm}$.

frequency between f_1 and f_2. The impedance bandwidth of CRMSA is found to be 3.27%. The simulated result of CRMSA is also shown in Figure 4.

Figure 5 shows the variation of return loss versus frequency of CTUAIURMSA when $U_w = 0.2\,\text{cm}$. The antenna resonates at seven modes of frequencies f_1, f_2, f_3, f_4, f_5, f_6 and f_7 with their respective impedance bandwidths $\text{BW}_1 = 3.18\%$ (3.4–3.51 GHz), $\text{BW}_2 = 4.81\%$ (3.65–3.83 GHz), $\text{BW}_3 = 6.56\%$ (5.6–5.98 GHz), $\text{BW}_4 = 10.625\%$ (6.06–6.74 GHz), $\text{BW}_5 = 7.44\%$ (7.63–8.22 GHz), $\text{BW}_6 = 6.25\%$ (8.22–8.75 GHz) and $\text{BW}_7 = 12.42\%$ (9.06–10.26 GHz). The first and second bands BW_1 and BW_2 are due to the fundamental resonance of the patch and the corner truncation, respectively. The remaining bands BW_3 and BW_7 are due to the insertion of U and inverted U-slots on the patch as they resonate independently. Further, it is seen from this figure that the construction of CTUAIURMSA does not much affect the primary resonant mode, i.e., f_1 (3.455 GHz) when compared to f_r (3.39 GHz) of CRMSA, but appears six additional resonating modes from f_2 to f_7. The simulated result of CTUAIURMSA is also shown in Figure 5 which is in good agreement for f_1 to f_4 with the experimental results.

Figure 6 shows the variation of return loss versus frequency of CTUAIURMSA when U_w is increased from 0.2 to 0.3 cm. It is clear from this figure that the antenna resonates for six resonating modes f_8, f_9, f_{10}, f_{11}, f_{12} and f_{13} having their respective impedance bandwidths of $\text{BW}_8 = 3.1\%$ (3.53–3.64 GHz), $\text{BW}_9 = 3.62\%$ (3.8–3.94 GHz),

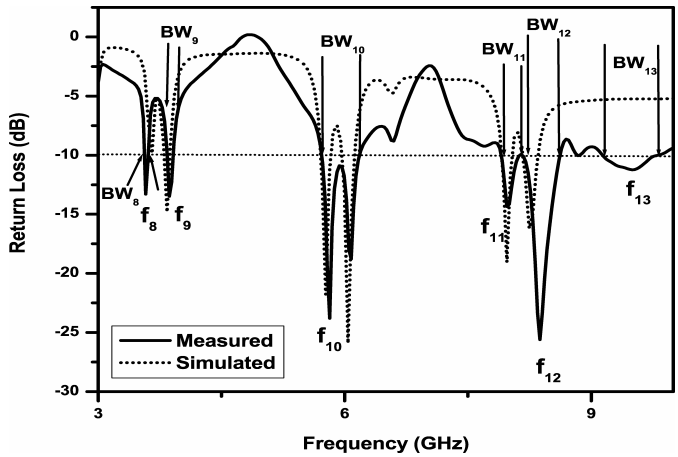

Figure 6. Variation of return loss versus frequency of CTUAIURMSA when $U_w = 0.3\,\text{cm}$.

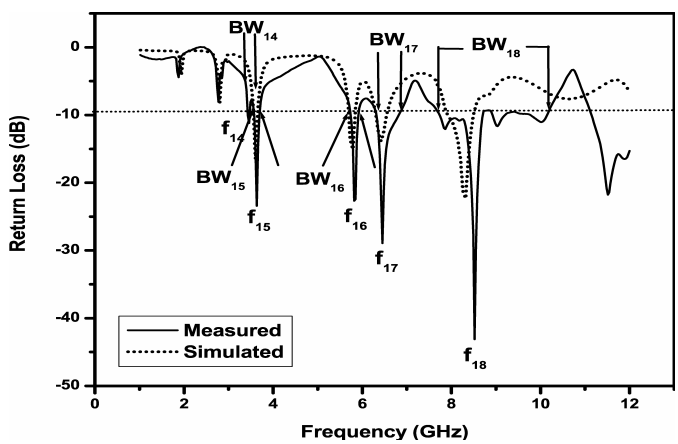

Figure 7. Variation of return loss versus frequency of CTUAIURMSA when $U_w = 0.1\,\text{cm}$.

$\text{BW}_{10} = 8.24\%$ (5.7–6.19 GHz), $\text{BW}_{11} = 3.25\%$ (7.87–8.13 GHz), $\text{BW}_{12} = 4.76\%$ (8.21–8.61 GHz) and $\text{BW}_{13} = 7.2\%$ (9.15–9.83 GHz) retaining the primary resonant mode f_8 (3.585 GHz) almost close to f_1 (3.445 GHz). The experimental return loss of CTUAIURMSA is in good agreement with simulated results as shown in Figure 6.

Figure 7 shows the variation of return loss versus frequency of CTUAIURMSA when U_w is decreased from 0.2 to 0.1 cm. It is noted from this figure that the antenna resonates for five resonating modes

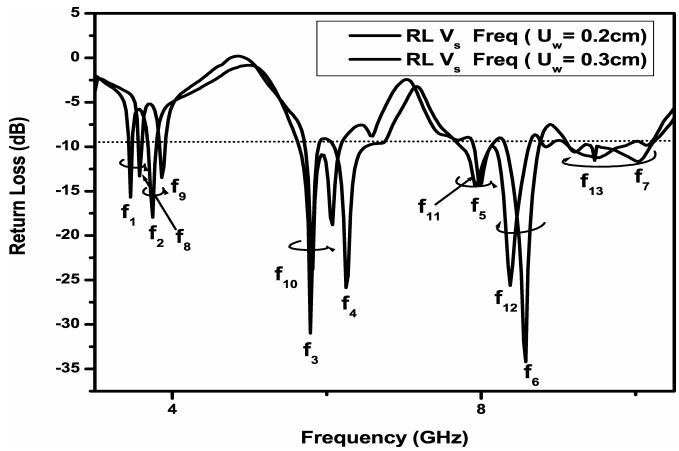

Figure 8. Comparison of experimental return loss versus frequency of CTUAIURMSA when $U_w = 0.2$ and 0.3 cm.

f_{14}, f_{15}, f_{16}, f_{17} and f_{18} having their respective impedance bandwidths of $BW_{14} = 2.9\%$ (3.4–3.5 GHz), $BW_{15} = 5.51\%$ (3.53–3.73 GHz), $BW_{16} = 4.5\%$ (5.68–5.94 GHz), $BW_{17} = 8.76\%$ (6.34–6.87 GHz) and $BW_{18} = 29.11\%$ (7.63–10.23 GHz). Further, it is noted that the primary resonant mode f_{14} (3.45 GHz) remains almost close to f_1 (3.445 GHz). The experimental return loss of CTUAIURMSA is in close agreement with simulated results.

Figure 8 shows the comparison of experimental return loss versus frequency of CTUAIURMSA when $U_w = 0.2$ and 0.3 cm. It is observed from this figure that when U_w is increased from 0.2 to 0.3 cm, the resonating modes f_8, f_9, f_{10} and f_{11} shown in Figure 8 are shifted towards higher frequency side compared to f_1, f_2, f_3 and f_5, respectively and f_{12} and f_{13} shifted towards lower frequency side compared to f_6 and f_7, respectively. This shift is due to the effect of increase in the width U_w from 0.2 to 0.3 cm of CTUAIURMSA.

Figure 9 shows the comparison of the experimental return loss versus frequency of CTUAIURMSA when $U_w = 0.1$ and 0.2 cm. It is noted from this figure that when U_w is decreased from 0.2 to 0.1 cm, the first resonating mode f_{14} almost remains unchanged compared to f_1, where as the modes f_{15} and f_{18} are shifted towards the lower frequency side compared to f_2 and f_6, respectively. The middle resonating modes f_{16} and f_{17} are shifted towards the higher frequency side compared to f_3 and f_4, respectively. This shifting of modes causes the bands BW_5, BW_6 and BW_7 shown in Figure 5 merge as a single band BW_{18} as shown in Figure 7, causing the enhancement in the impedance band width of about 29.11%. The shifting of the bands and improvement

in the impedance bandwidth are due to the decrease of U_w from 0.2 to 0.1 cm. The current along the edges of the slots introduces an additional resonance, resulting in enhancement in the impedance bandwidth of the antenna [22]. Hence by varying the width the U and inverted U-slot, i.e., U_w, modes of CTUAIURMSA can be tuned in either side of the frequency spectrum, without much affecting the

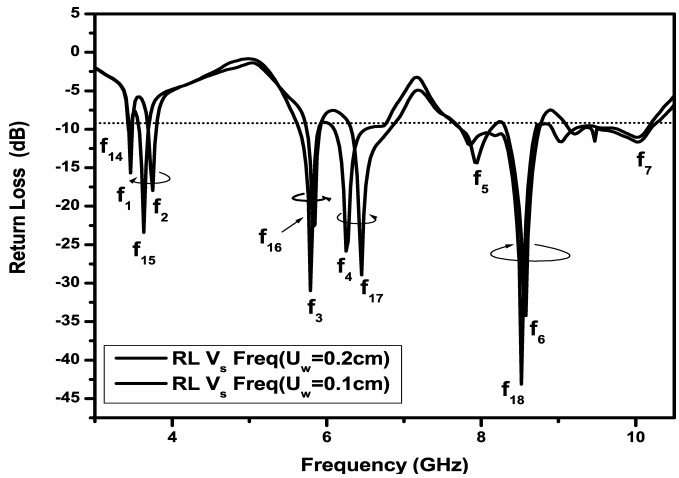

Figure 9. Comparison of experimental return loss versus frequency of CTUAIURMSA when $U_w = 0.2$ and 0.1 cm.

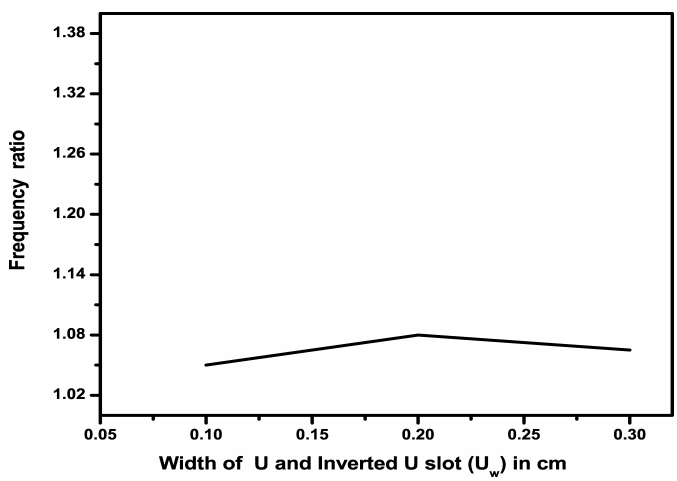

Figure 10. Variation of frequency ratio versus width (U_w) of CTUAIURMSA.

primary resonant mode. The variation of U_w changes the coupling effect on the corner truncation of patch, U and inverted U-slots, which causes the shift of bands towards upper and lower frequency sides. Further, CTUAIURMSA uses less copper area of 69.85% compared to copper area of CRMSA by loading U and inverted U-slots and corner truncation of the radiating patch.

Figure 10 shows the variation of frequency ratio f_2/f_1 when $U_w = 0.2\,\text{cm}$, f_9/f_8 when $U_w = 0.3\,\text{cm}$ and f_{15}/f_{14} when $U_w = 0.1\,\text{cm}$ versus width (U_w) of CTUAIURMSA. From this figure, it is clear that the frequency ratio remains almost equal to 1.06, indicating not much variation in the primary resonant mode of the antenna.

The co-polar and cross-polar radiating patterns of CRMSA, CTUAIURMSA measured in their matched bands are shown in Figures 11 to 29. From these figures, it can be observed that the patterns are broadside and linearly polarized. The highest cross polar power level is $-15\,\text{dB}$ down compared to their co-polar power level.

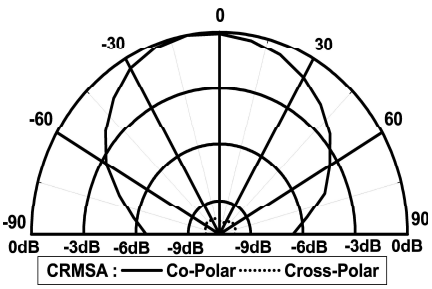

Figure 11. Radiation pattern of CRMSA measured at 3.39 GHz.

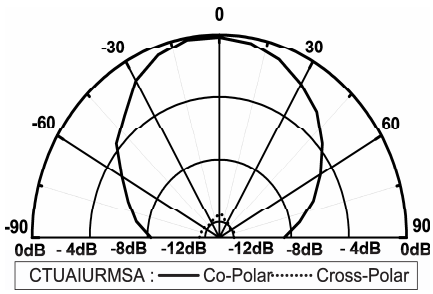

Figure 12. Radiation pattern of CTUAIURMSA when $U_w = 0.2\,\text{cm}$ measured at 3.445 GHz.

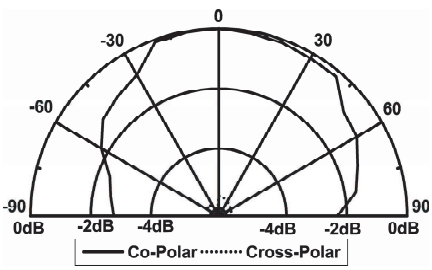

Figure 13. Radiation pattern of CTUAIURMSA when $U_w = 0.2\,\text{cm}$ measured at 3.74 GHz.

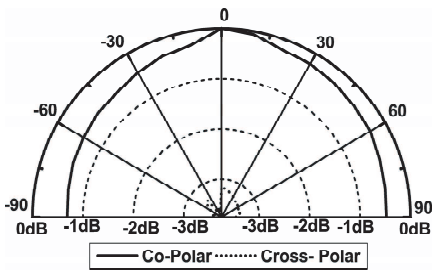

Figure 14. Radiation pattern of CTUAIURMSA when $U_w = 0.2\,\text{cm}$ measured at 5.79 GHz.

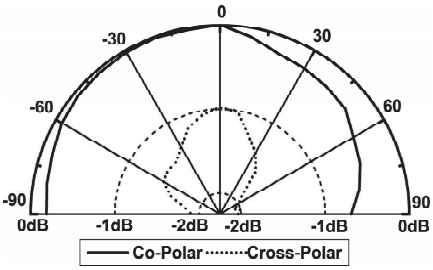

Figure 15. Radiation pattern of CTUAIURMSA when U_w = 0.2 cm measured at 6.4 GHz.

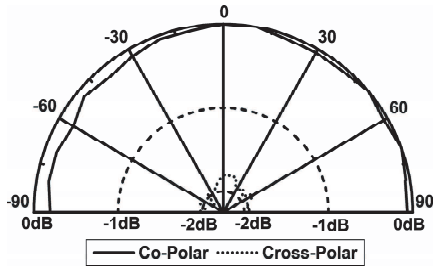

Figure 16. Radiation pattern of CTUAIURMSA when U_w = 0.2 cm measured at 7.925 GHz.

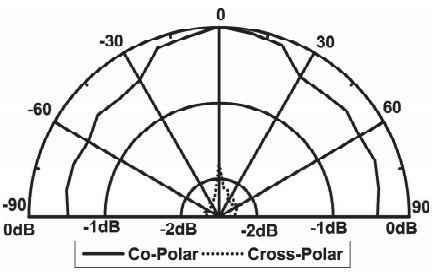

Figure 17. Radiation pattern of CTUAIURMSA when U_w = 0.2 cm measured at 8.485 GHz.

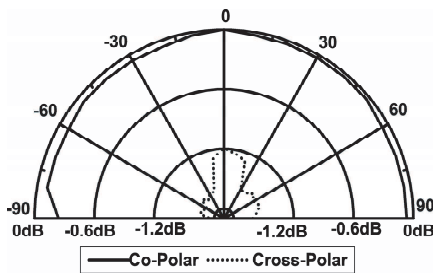

Figure 18. Radiation pattern of CTUAIURMSA when U_w = 0.2 cm measured at 9.66 GHz.

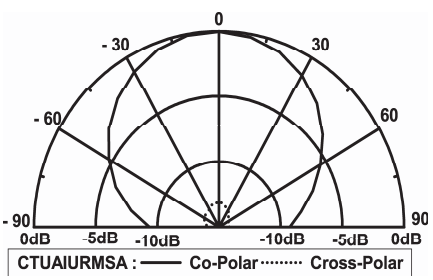

Figure 19. Radiation pattern of CTUAIURMSA when U_w = 0.3 cm measured at 3.585 GHz.

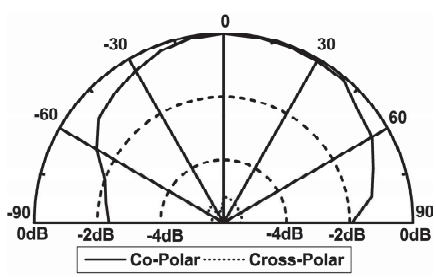

Figure 20. Radiation pattern of CTUAIURMSA when U_w = 0.3 cm measured at 3.82 GHz.

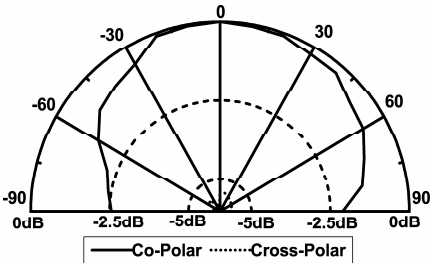

Figure 21. Radiation pattern of CTUAIURMSA when U_w = 0.3 cm measured at 5.945 GHz.

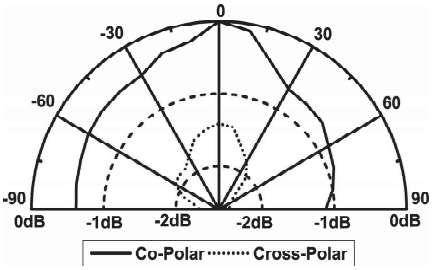

Figure 22. Radiation pattern of CTUAIURMSA when U_w = 0.3 cm measured at 8.0 GHz.

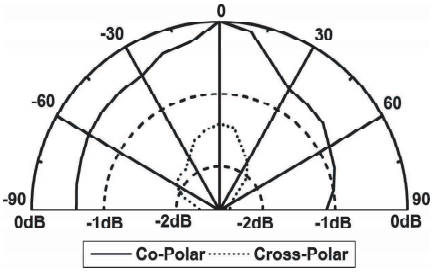

Figure 23. Radiation pattern of CTUAIURMSA when U_w = 0.3 cm measured at 8.41 GHz.

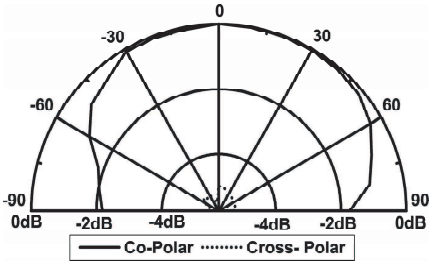

Figure 24. Radiation pattern of CTUAIURMSA when U_w = 0.3 cm measured at 9.49 GHz.

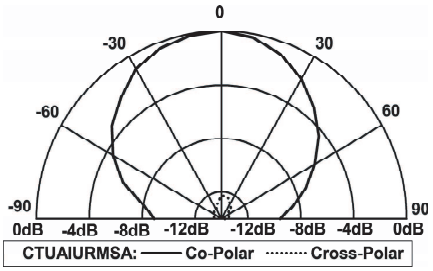

Figure 25. Radiation pattern of CTUAIURMSA when U_w = 0.1 cm measured at 3.45 GHz.

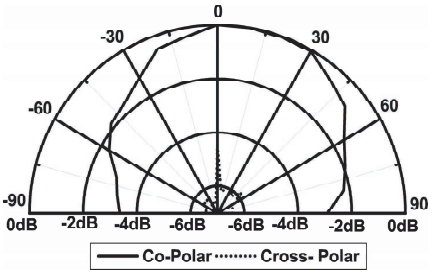

Figure 26. Radiation pattern of CTUAIURMSA when U_w = 0.1 cm measured at 3.63 GHz.

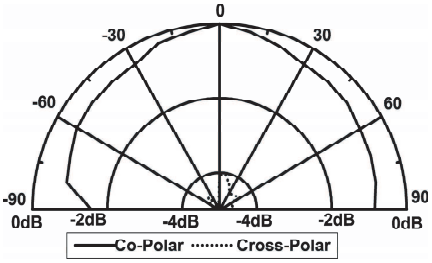

Figure 27. Radiation pattern of CTUAIURMSA when $U_w = 0.1\,\text{cm}$ measured at 5.81 GHz.

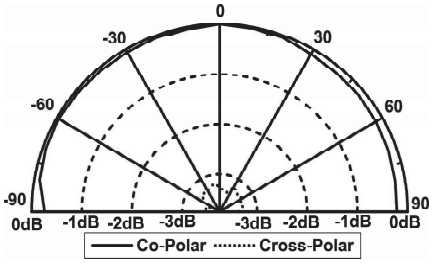

Figure 28. Radiation pattern of CTUAIURMSA when $U_w = 0.1\,\text{cm}$ measured at 6.05 GHz.

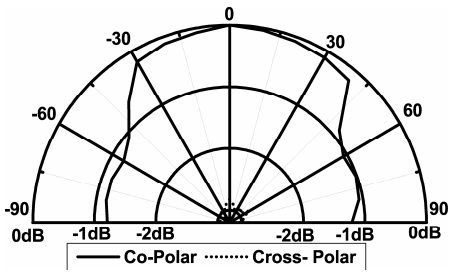

Figure 29. Radiation pattern of CTUAIURMSA when $U_w = 0.1\,\text{cm}$ measured at 8.93 GHz.

Table 2. Gains of matched bands.

Matched Band	Gain (dB)	Matched Band	Gain (dB)	Matched Band	Gain (dB)
BW_1	1.64	BW_7	0.27	BW_{13}	0.38
BW_2	0.75	BW_8	1.66	BW_{14}	1.68
BW_3	0.57	BW_9	1.63	BW_{15}	1.73
BW_4	0.44	BW_{10}	0.64	BW_{16}	0.45
BW_5	0.68	BW_{11}	0.66	BW_{17}	0.15
BW_6	0.18	BW_{12}	1	BW_{18}	1.13

The gain of CRMSA and CTUAIURMSA is calculated using the absolute gain method given by the relation,

$$(G)\,\text{dB} = 10\log\left(\frac{P_r}{P_t}\right) - (G_t)\,\text{dB} - 20\log\left(\frac{\lambda_0}{4\pi R}\right)\,\text{dB} \tag{2}$$

where, G_t is the gain of the pyramidal horn antenna and R the

distance between the transmitting antenna and the antenna under test (AUT). The power received by AUT, 'P_r' and the power transmitted by standard pyramidal horn antenna 'P_t' are measured independently. The maximum gain measured at each matched band BW_1 to BW_{18} is given in Table 2. The antenna gives the highest measured gain of 1.73 dB. The highest simulated gain is 1.4 dB, close to the measured gain.

4. CONCLUSION

From the detailed study, it is found that the CRMSA can be made to operate at different bands between 3 to 12 GHz by loading U and inverted U-slot on the radiating patch. The insertion of U and inverted U-slots also enhances the gain from 0.90 to 1.73 dB. The multi bands of CTUAIURMSA gives almost constant frequency ratio, and the resonating bands can be tuned on either side of the frequency spectrum by changing the width of horizontal and vertical arms of U and inverted U-slot without affecting the primary band. Tuning of multibands does not affect the nature of broadside radiation characteristics. The proposed antennas are simple in their geometry and fabricated using low cost glass epoxy substrate material. These antennas may find applications in WiMax (3.4 to 3.6 GHz), WiMax of IEEE802.16d (5.7–5.9 GHz), HIPERLAN/2 (5.725 to 5.825 GHz) and radar communication systems.

ACKNOWLEDGMENT

The authors would like to thank the Department of Science and Technology (DST), Government of India, New Delhi, for sanctioning Vector Network Analyzer to this Department under FIST project.

REFERENCES

1. Kumar, G. and K. P. Ray, *Broadband Microstrip Antennas*, Artech House, Norwood, MA, 2003.
2. Chulvanich, C., J. Nakasuwan, N. Songthanapitak, N. Anantrasirichai, and T. Wakabayashi, "Design narrow slot antenna for dual frequency," *PIERS Online*, Vol. 3, No. 7, 1024–1028, 2007.
3. Archevapanich, T., J. Nakasuwan, B. Purahong, N. Anantrasirichai, and O. Sangaroon, "Inset dual U-strip slot antenna fed by microstrip line for WLAN applications,"

International Conference on Control, Automation and Systems, 1785–1788, Seoul, Korea, 2008.

4. Wi, S. H., Y. B. Sun, I. S. Song, S. H. Choa, I. S. Koh, Y. S. Lee, and J. G. Yook, "Package-level integrated antennas based on LTCC technology," *IEEE Trans. Antennas Propagat.*, Vol. 54, No. 8, 2190–2197, 2006.
5. Kasbegoudar, V. G. and K. J. Vinoy, "A broadband suspended microstrip antenna for circular polarization," *Progress In Electromagnetic Research*, Vol. 90, 353–368, 2009.
6. Islam, M. T., M. N. Shakib, and N. Misran, "Multi-slotted microstrip patch antenna for wireless communication," *Progress In Electromagnetics Research Letters*, Vol. 10, 11–18, 2009.
7. Ray, K. P., S. Ghosh, and K. Nirmala, "Multilayer multi-resonator circular microstrip antenna for broad band and dual band operations," *Microwave and Optical Technology Letters*, Vol. 47, 489–494, Dec. 2005.
8. Wang, F. J. and J.-S. Zhang, "Wideband cavity-backed patch antenna for PCS/IMT2000/2.4 GHz WLAN," *Progress In Electromagnetic Research*, Vol. 74, 39–46, 2007.
9. Sharma, A. and G. Singh, "Design of single pin shorted three-dielectric layered substrates rectangular patch microstrip antenna for communication system," *Progress In Electromagnetic Research Letters*, Vol. 2, 157–165, 2008.
10. Kuo, J. S. and K. L. Wong, "A compact microstrip antenna with meandered slots in the ground plane," *Microwave and Optical Technology Letters*, Vol. 29, 95–97, Apr. 2001.
11. Eldek, A. A., A. Z. Elsherbeni, and C. E. Smith, "Characteristics of bow-tie slot antenna with tapered tuning stubs for wideband operation," *Progress In Electromagnetics Research*, Vol. 49, 53–69, 2004.
12. Ang, B.-K. and B.-K. Chung, "A wideband E-shaped microstrip patch antenna for 5–6 GHz wireless communication," *Progress In Electromagnetics Research*, Vol. 75, 397–407, 2007.
13. Waterhouse, R. B., "Broadband stacked shorted patch," *Electronic Letters*, Vol. 35, 98–100, Jan. 1999.
14. Ge, Y., K. P. Esselle, and T. S. Bird, "A broadband E-shaped patch antenna with a microstrip compatible feed," *Microwave and Optical Technology Letters*, Vol. 42, No. 2, Jul. 2004.
15. Nishiyama, E. and M. Aikawa, "Wide-band and high gain microstrip antenna with thick parasitic patch substrate," *IEEE Antennas and Propagat., Int. Soc. Symp.*, 273–276, 2004.

16. Levine, E., G. Malamud, S. Shtrikman, and D. Treves, "A study of microstrip array antennas with the feed network," *IEEE Trans. Antennas Propagat.*, Vol. 37, 426–434, 1989.
17. Behera, S. and K. J. Vinoy, "Microstrip square ring antenna for dual-band operation," *Progress In Electromagnetics Research*, Vol. 93, 41–56, 2009.
18. Roy, J. S., N. Chattoraj, and N. Swain, "Short circuited microstrip antenna for multi-band wireless communications," *Microwave and Optical Technology Letters*, Vol. 48, 2372–2375, 2006.
19. Sadat, S., M. Fardis, F. G. Gharakhili, and G. R. Dadashzadeh, "A compact microstrip square-ring slot antenna for UWB applications," *Progress In Electromagnetics Research*, Vol. 67, 173–179, 2007.
20. Shams, K. M. Z., M. Ali, and H. S. Hwang, "A planar inductively coupled bow-tie slot antenna for WLAN application," *Journal of Electromagnetic Waves and Applications*, Vol. 20, No. 7, 861—871, 2006.
21. Bahl, I. J. and P. Bhartia, *Microstrip Antennas*, Artech House, New Delhi, 1980.
22. Rafi, G. Z. and L. Shafai, "Wideband V-slotted diamond-shaped microstrip patch antenna," *Electronics Letters*, Vol. 40, No. 19, 1166–1167, 2004.